Ann. Occup. Hyg., Vol. 56, No. 6, pp. 645–659, 2012

doi:10.1093/annhyg/mer123

An Inter-Laboratory Study to Determine the Effectiveness of Procedures for Discriminating Amphibole Asbestos Fibers from Amphibole Cleavage Fragments in Fiber Counting by Phase-Contrast Microscopy

MARTIN HARPER[1]*, EUN GYUNG LEE[1], JAMES E. SLAVEN[2,4] and DAVID L. BARTLEY[3]

[1]Exposure Assessment Branch, Health Effects Laboratory Division, National Institute for Occupational Safety and Health, 1095 Willowdale Road, MS-3030, Morgantown, WV 26505, USA; [2]Biostatistics and Epidemiology Branch, Health Effects Laboratory Division, National Institute for Occupational Safety and Health, 1095 Willowdale Road, MS-4050, Morgantown, WV 26505, USA; [3]3904 Pocahontas Avenue, Cincinnati, OH 45227, USA

Received 15 July 2011; in final form 8 December 2011; published online 28 March 2012

The US Occupational Safety and Health Administration (OSHA) and Mine Safety and Health Administration do not regulate cleavage fragments of amphibole and serpentine minerals as asbestos, even when particles meet the dimensional criteria for counting under standard phase-contrast microscopy methods. The OSHA ID-160 method cautions that discriminatory counting is difficult and should not be attempted unless necessary and no procedure is provided for differentiation. A standard published by the American Society for Testing and Materials (ASTM International D7200-06) includes an attempt to codify a procedure but recognizes that the procedure should be validated in an inter-laboratory study. The US National Institute for Occupational Safety and Health has carried out such a study with multiple laboratories using slides made from riebeckite and crocidolite, grunerite and amosite, tremolite and tremolite asbestos, and actinolite and actinolite asbestos using two different measurement aids (graticules). The asbestos fibers had dimensions consistent with those reported for air samples from actual amphibole asbestos operations, and the cleavage fragments were also dimensionally consistent with those found in non-asbestos mining and milling operations. The procedure for discriminating asbestos fibers from other mineral particles in the ASTM Standard calls for the recognition of characteristics supposedly common to asbestos. For the asbestos fibers created in this study, these characteristics were found not to be common and generally a function of length. More importantly, different laboratories did not recognize these features consistently. Laboratories were much more consistent in measuring dimensions, but excessive overlap in the lengths of asbestos fibers and cleavage fragments rendered length a poor criterion for discrimination. The ASTM discrimination procedure as written could not be supported on the basis of this study. Width was a much more consistent parameter for distinguishing the asbestos and non-asbestos fibers in this study and inclusion of aspect ratio, while considered important by some researchers, did not refine the discrimination further. The ability of the majority of microscopists in this study to discriminate fibers and cleavage fragments through measurement of particle widths was determined and found to be within limits of uncertainty typical for air sampling measurements. A width criterion might be a very simple and useful aid where discrimination between asbestos and non-asbestos fibers in fiber counting by phase-contrast microscopy is required for further

*Author to whom correspondence should be addressed. Tel: +1-304/285-5823; fax: +1-304/285-6034; e-mail: mharper@cdc.gov
[4]Present address: Biostatistics Department, HS-3000, Indiana University-Purdue University, Indianapolis, IN 46202, USA

investigation. Recognition of asbestos features can also be retained as excessive recognition by some laboratories will lead to a conservative decision for additional investigation.

Keywords: amphibole cleavage fragments; asbestos analysis; fiber measurement; inter-laboratory study; phase-contrast microscopy

INTRODUCTION

Amphibole minerals are found in many geological environments. Amphiboles may crystallize in massive, prismatic, or fibrous habits. One fibrous habit of considerable importance is that which gives rise to asbestos and hence is described as asbestiform. The asbestiform habit is characterized by parallel growth of crystals with large aspect ratios, which is to say widths in the nanometer scale and lengths in micrometers or longer. The individual crystals have been termed fibrils. The parallel growth of fibrils leads to bundles (fibrillar bundling). The term 'fiber' has been applied at every scale and thus is an awkward term to define with scientific accuracy. Most asbestos fibers observed at the magnification of the light microscope and all that can be seen under the naked eye are such bundles of fibrils. In regulation, fiber has been given a more exact definition based on dimensional criteria only, and the definition of fiber in this paper is based on the US National Institute for Occupational Safety and Health (NIOSH) Method 7400 'A' counting rules, i.e. aspect ratio (length/width) $\geq$3:1 and length $>$5 μm (NIOSH, 2003a), along with the World Health Organization (WHO, 1997) counting rule for width ($<$3 μm), which is not part of the NIOSH Method 7400 'A' rules but which is included in the NIOSH 'B' counting rules. Mining, crushing, processing, and using any minerals generally causes dust to form and rise into the air. Airborne mineral dust is subject to occupational and environmental regulation, depending on the nature of the mineral. Asbestos dust regulation is based on counting the number of fibers that are collected on a membrane filter, most often under an optical microscope, which has advantages of portability, speed, and cost over microscopes with greater magnification.

A problem in distinguishing amphibole asbestos, especially in airborne dust samples at the magnification of the light microscope, is that amphibole crystals developed in other habits may resemble asbestos in fibrillar bundles or may break by cleavage into fragments whose size overlaps that of the asbestos fibers visible at the same magnification. Such fine prismatic crystals and cleavage fragments are not regulated as asbestos by the US Occupational Safety and Health Administration (OSHA) or the Mine Safety and Health Administration (MSHA) (OSHA, 1992; MSHA, 2005). However, the current position of NIOSH and the Environmental Protection Agency (EPA, 2003) is that cleavage fragments should be included in fiber counts. One of the reasons put forward for the NIOSH position (but not the only one) is the difficulty of distinguishing amphibole asbestos from prismatic crystals or cleavage fragments, especially where they might occur together. OSHA also admits this difficulty and thus discourages attempts to distinguish these crystalline forms, 'unless it is legally necessary' (OSHA, 1988, revised 1997). In recent years, the American Society for Testing and Materials (ASTM International) has published a standard, *D7200-06 Standard Practice for Sampling and Counting Airborne Fibers, Including Asbestos Fibers, in Mines and Quarries, by Phase Contrast Microscopy and Transmission Electron Microscopy* (ASTM International, 2006), which includes a procedure for determining whether the particles observable under phase-contrast microscopy meeting the definition of a fiber are likely to be asbestiform fibers or cleavage fragments (or possibly also fine prismatic crystals, although this is not stated). The procedure for discrimination involves the appearance of asbestiform features, such as curvature, split ends or fibrillar bundling (Class 1), and dimensional criteria (Class 2: length $>$10 μm or width $<$1 μm). Standard D7200-06 includes the statement: '16.2.6 The intra-microscopist and inter-microscopist precision of differential fiber counting has not been established, and may be larger than the values encountered in fiber identification alone. It is the intention of the ASTM committee responsible for this practice to encourage an investigation of this issue at the earliest possible date, and to ballot to withdraw this practice from publication if an acceptable precision is not established within a reasonable period of time'. Thus, an ASTM Inter-laboratory study (ILS #0282) was registered for the purpose providing precision as well as bias and accuracy. This paper reports on the conduct and results of the ILS.

Materials and methods

The selection of standard materials for these tests has already been described (Harper *et al.*, 2007,

2008). Riebeckite crystals were collected from a type locality; grunerite and actinolite from type localities were purchased from mineral dealers; tremolite from a prior project was already available. The raw materials that became the US National Institute for Standards and Technology (NIST) standards for crocidolite and amosite were already available and reference tremolite asbestos and actinolite asbestos were donated from the repository of the Health and Safety Laboratory (UK). The NIST amosite and crocidolite samples were specially selected in the preparation process to be 'bundles approaching 6 cm in length' and were considered to be '>90%' asbestos (NIST, 1991). We believe that the subsequent processing of these materials for this study would have further concentrated asbestos fibers, if further concentration was needed, to produce a product so close to 100% asbestos that it can be so-termed. Each material was processed at Research Triangle Institute (RTI International, Research Triangle Park, NC) to prepare the maximum number of particles according to the definition of fiber given above. Preparation of the non-asbestiform cleavage fragments has been described previously (Harper *et al.*, 2007, 2008), but a more detailed description of the preparation of the asbestos analogs is given below. Because each candidate asbestiform material had been previously milled or otherwise processed, further processing for the purposes of this study involved only the amount of additional ball milling necessary to generate fibers in the general dimensional range described above. For each asbestiform material, an aliquot of 0.6 g was weighed using a Mettler PG 502 balance and that aliquot was placed in a Spex tungsten carbide ball mill sample holder and mechanically milled for 5 min. A glass slide mount was prepared with the mineral and 1.550 refractive index liquid (to provide maximum relief). The slide was then inspected using polarized light microscopy. After each subsequent 1-min interval, another slide mount was made and labeled with the asbestos type and the cumulative amount of milling time it had been ground, until the powder was notably overmilled, i.e. when the fibrous nature is lost. (The material had been reduced to microscopic particles with very low (2:1–1:1) aspect ratios and agglomerations of non-fibrous particles). This typically occurred at ~17 min total milling time. Each slide preparation to this point was then examined in order to determine the optimal milling time necessary to render particles best meeting the previously stated study goals. The optimal total milling time was recorded and four to six aliquots of 0.6 g were weighed for mass production of the asbestiform material needed for later phases of the study. Each different asbestos type was ground for the appropriate amount of time, and one vial (2–3 g final weight) of each milled asbestiform material was reserved for suspension, filtration, and eventual characterization by phase-contrast microscopy and transmission electron microscopy. Each milled material was given an initial examination and imaged by polarized light microscopy, scanning electron microscopy, and transmission electron microscopy. For each of the four asbestiform minerals, ~0.6 g of milled material was placed in a 400-ml beaker with 120 ml of distilled water and 60 ml of isopropyl alcohol. The suspension was stirred and sonicated using an ultrasonic dismembrator for ~12 to 15 min. The suspension was then poured into a 2-l graduated cylinder (75 mm diameter × 420 mm deep at the 2 l mark) with 5 ml of 10% acetic acid as dispersant, topped off to 2 l, and stirred for 5 min. When the stirring was stopped and the swirling of particles ceased, a timer was started. After 30 min of settling, a 5 ml aliquot was withdrawn from the 600 ml level of the cylinder (126 mm above base) and diluted to 250 ml This procedure is based on a standard operating procedure for separating asbestos fibers from soils (Brattin and Orr, 2004). Subaliquots in volumes ranging from 0.1 to 5.0 ml were then deposited on 25 mm diameter 0.45-μm pore size mixed cellulose ester filters using a six-station filter manifold. After the filters were dried, quarters of each filter were placed on glass slides and collapsed using an acetone vaporizer. The preparations were sealed with cover slips and triacetin. Particle densities from each subaliquot volume were assessed to ensure that they were appropriate and then six additional aliquots from the optimal subaliquot volume were filtered and prepared, as above, for analysis by phase-contrast microscopy and transmission electron microscopy. The particle analysis results were published previously (Harper *et al.*, 2008) and were considered to be consistent with previously published analyses (Gibbs and Hwang, 1980; Virta *et al.*, 1983) of airborne particles collected on filters in workplaces.

Suspensions were made and used to prepare reference slides that contained mixtures of asbestos fibers and cleavage fragments of the same amphibole. One set of slides contained 100% asbestos, while another contained 100% cleavage fragments. Mixtures were also prepared to give nominal ratios of 60:40 and 20:80 asbestos to cleavage fragments. However, there is no way to independently confirm the exactness of those ratios. Slides sets were prepared with both a low and a high total loading. Low loadings were in the range of 50–400 fibers mm^{-2}, and the high loadings were in the range of 250–1300 fibers

mm^2, as determined by phase-contrast microscopy. Slides were prepared using the dimethylformamide solution/Euparal mounting method as this has been shown to ensure the long-term permanence of fiber positions and covered with a coverslip containing a relocatable grids supplied by Thomas Pang (Ryerson University, Ontario, Canada). Drawings of the fibers observable in each field were made and on each slide ~100 fibers meeting the required dimensional criteria were identified. The slides and accompanying documentation were sent out to the participating laboratories in the ILS in two parts. The first part involved the slides of riebeckite/crocidolite and grunerite/amosite and involved nine laboratories. The laboratories were asked to examine the slides under phase-contrast microscopy and determine for each labeled particle whether it met the definition of Class 1 of the ASTM procedure, i.e. did it exhibit curvature, split ends, or fibrillar bundling. Then, they were asked to determine the length and width to the nearest 0.1 μm so that the procedure for determining Class 2 of the ASTM procedure could be evaluated. The laboratories were asked to perform this measurement using the Walton–Beckett graticule (Fig. 1). For the first part of the study, they were also asked to examine the slides using the RIB graticule (Fig. 2) manufactured by Klarmann Rulings (Litchfield, NH, USA), which was supplied to each laboratory. Further details concerning the RIB graticule (RIB is a trade name without particular meaning as an acronym) may be found in the ASTM Standard. Each laboratory was asked to ensure that the same microscopist examined all slides. One laboratory was unable to do this but results from the two microscopists did not appear to be different and so were combined. Telephone interviews were used to ensure all laboratories properly understood the written procedures. In the second part of the project, the tremolite/tremolite asbestos and actinolite/actinolite asbestos slides were sent out. One laboratory dropped out of the study after the first part, but two more were added in the second to bring the total for that part to 10 (thus, 11 laboratories participated in at least one part). Since results from the first part of the study indicated no significant difference between the two graticules, laboratories were asked only to use the Walton–Beckett graticule in the second part of the study.

RESULTS

Measurements

With very large numbers of measurements (~100 particles × 32 slides = ~3200 measurements in each laboratory) and variance about the mean being small, most laboratories can be shown to be statistically different in their measurements from each other for width measurements because of the large proportional difference of even a small deviation. On the other hand, there was almost no difference between most laboratories for length measurements, except for one laboratory which was significantly different from nearly all other laboratories for nearly all materials and which was also one that experienced difficulty with width measurements as described below. The inter-laboratory variance in width would be best explored if there was a robust true measurement, but there is not. In this case, it is necessary to compare the individual laboratories width measurements to the mean of all laboratories (as for example, is done in the proficiency test program of the American Industrial Hygiene Association). This is shown in Table 1. Although two of the laboratories (#2 and #9) had means that deviated by ≥15% from the group means, there was no significant difference for any laboratory against the mean of all laboratories discernable by any statistical methods we employed, which included analysis of variances (ANOVAs) using actual width measurements to test between laboratories; ANOVAs to look at differences in ratio, as measured by laboratory values divided by overall means; *t*-tests to look for differences between laboratory measures and the overall mean of all laboratories combined; Bland–Altman graphing techniques; and the Tietjen–Moore test for rejecting outlier pairs. Interestingly, there was no significant difference in measurements made using the Walton–Beckett graticule as compared to the RIB graticule, and Bland–Altman plots showed no constant trend. However, in the case of the two laboratories that have the most different width measurements from the mean of all laboratories, the mean ratios were considerably closer to unity with the RIB graticule than with the Walton–Beckett graticule (Table 2). This might be anticipated since the RIB graticule has gradations at 0.5 and 1.0 μm specifically to aid these finer measurements, while the smallest gradations of the Walton–Beckett graticule are at 3.0 μm. Another explanation may simply be the introduction of a novel procedure causing greater attention to detail in the measurements by these laboratories. Nevertheless, the overall ability of microscopists to measure width is good, especially ~1 μm, and the results from measurements with the Walton–Beckett graticule from all laboratories were used in the data interpretation. The accuracy of the measurement of a single fiber width in any given size range may be calculated (Appendix 1).

Class 1 detection. The average results for the 100% asbestos slides and the 0% asbestos (100%

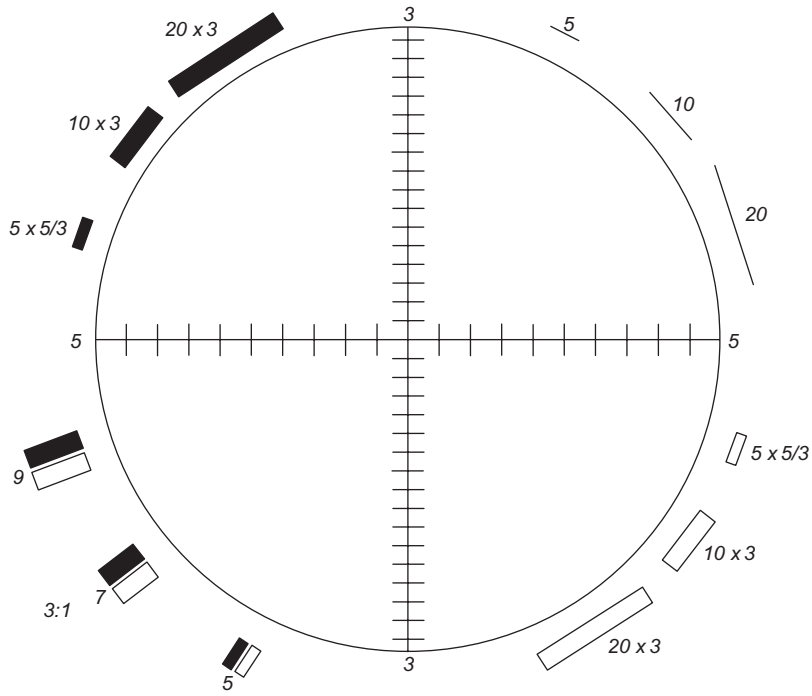

Fig. 1. Walton–Beckett graticule.

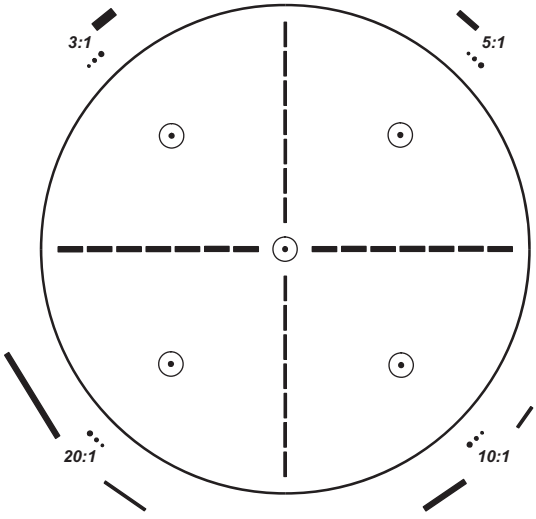

Fig. 2. RIB graticule (RIB is a trade name without particular meaning as an acronym).

cleavage fragment) slides are shown in Table 3 (the results for the other slides followed a similar pattern but have been omitted for clarity). The range of identification of Class 1 characteristics was from 0 to 96% for the asbestos-only slides and <1–85% for the non-asbestos slides. This degree of overlap effectively ensures that the recognition of Class 1 characteristics cannot be used across laboratories to distinguish asbestos fibers from cleavage fragment particles. Even for crocidolite, which is generally considered to most embody the 'asbestiform' characteristics, recognition rates varied from 0 to 52% and most participants identified <10% of the other types of asbestos fibers as having Class 1 characteristics. Since it is possible that the sample preparation may have reduced the size of bundles or reduced the appearance of split ends, to the point where the particles are no longer recognized as bundles, the identification of Class 1 characteristics was further investigated. A regression line can be plotted between particle length and probability of recognition of Class 1 features for any slide containing 100% asbestos and the clearest example of this relationship is given in Fig. 3. The absence of recognition of Class 1 characteristics appears to be a reflection of the actual absence of those characters, especially for shorter fibers, i.e. the shorter the fiber the less likely it is to show bundling, split ends, and curvature. This may be because curvature and splits in the ends are present but below the limit of visual detection or that these features are absent for some reason of crystal habit. Fibers that are >10 μm would be recognized as asbestos under Class 2 parameters, but many of our fibers were in the range 5–10 μm, which is consistent with published size distributions

Table 1. Ratio of width measurements to the mean width measurements of all laboratories.

Laboratory #	1	2	3	4	5	6	7	8	9	10	11
CR	1.04	0.67	0.94	0.99	0.97	1.12	1.01	1.01	1.26	—	—
AG	1.06	0.66	0.92	1.00	0.95	1.15	1.06	0.96	1.24	—	—
TR	1.11	0.82	0.89	0.97	0.96	1.14	—	1.00	1.11	1.05	0.96
AC	1.07	0.84	0.90	0.92	0.96	1.08	—	1.03	1.20	1.08	0.93

Note that the deviations >15% for Laboratories 2 and 9 are not significant, just large. Mean ratio of all particles on all slides for each different amphibole class (key: CR, crocidolite/riebeckite; AG, amosite/grunerite; TR, tremolite asbestos/tremolite; AC, actinolite asbestos/actinolite) measured with Walton–Beckett graticule.

Table 2. Ratio of width measurements to the mean width measurements of all laboratories for RIB versus WB graticules.

Laboratory #	1	2	3	4	5	6	7	8	9	10	11
CR (WB)	1.04	0.67	0.94	0.99	0.97	1.12	1.01	1.01	1.26	—	—
CR (RIB)	1.08	0.78	0.98	0.92	0.97	1.16	0.94	1.02	1.14	—	—
AG (WB)	1.06	0.66	0.92	1.00	0.95	1.15	1.06	0.96	1.24	—	—
AG (RIB)	1.07	0.77	0.96	0.91	0.99	1.18	0.99	1.02	1.11	—	—

Note the distinct improvement of results for Laboratories 2 and 9 when using the RIB graticule compared to the Walton–Beckett graticule (WB). Otherwise, key as Table 1.

Table 3. Proportion of Class 1 identification in 100 and 0% asbestos slides.

Laboratory	100% Asbestos fibers				0% Asbestos fibers			
	CR	AG	TR	AC	CR	AG	TR	AC
1	25	6.2	2.2	0	2.3	5.9	6.7	4.5
2	9.9	11	13	8.9	34	34	71	85
3	14	2.0	2.9	0.4	1.4	0.9	1.3	1.1
4	9.5	3.7	1.7	1.8	0.9	4.1	1.0	1.0
5	52	19	8.2	2.6	11	11	8.1	1.0
6	18	0.5	9.3	1.7	1.4	1.6	16	23
7	39	13	—	—	17	13	—	—
8	46	24	15	28	8.8	4.5	20	5.8
9	46	36	29	32	73	57	71	85
10	—	—	90	96	—	—	11	0.6
11	—	—	3.5	10	—	—	7.9	2.4

Each result is the average of the low and high loading slides. Key as in Table 1.

of particles from workplace amphibole asbestos samples. These fibers would not likely be recognized as Class 1 or Class 2. The reverse situation is also cause for concern. Some laboratories correctly identified ≤1% Class 1 characteristics in the slides with no asbestos fibers but others counted up to 85%. Laboratory #2 and laboratory #9 recognized a greater percentage of Class 1 features in the cleavage fragments slides than in the asbestos slides, and it is likely that they were classifying cleavage fragments as thick asbestos fiber bundles. On the other hand, laboratory #10 identified an improbably high number of objects in the asbestos slides as having Class 1 characteristics and it is likely that they were including the narrower width of these fibers as a characteristic even though this was not part of the instruction.

Class 2 detection. As noted in a previous publication (Harper *et al.*, 2007), many of the cleavage fragments in our preparations were >10 μm, which is nonetheless consistent with dimensions of particles in air samples from workplaces where cleavage fragments are known to be present (see review in Harper *et al.*, 2008). Identifying a substantial portion of cleavage fragments as asbestos fibers defeats the object of the procedure. Also, as noted previously, a significant portion of asbestos fibers is <10 μm and this

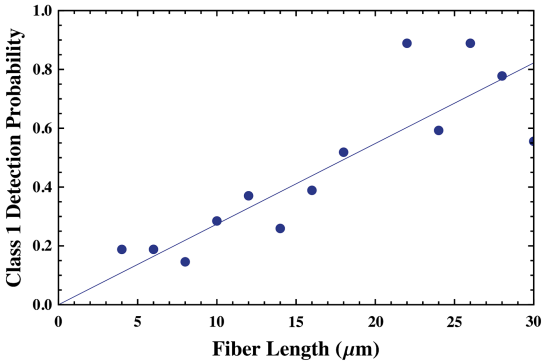

Fig. 3. Relationship of fiber length to recognition of asbestiform morphology (Class 1 detection) in one of the 100% crocidolite slides. Points represent individual fibers on the slide recognized as Class 1 by at least one laboratory.

Table 4. Proportion of fibers selected for measurement in slides prepared for the ILS meeting the criterion of ≤1 μm width.

Nominal percentage asbestos (%)	CR % ≤1 μm	AG % ≤1 μm	TR % ≤1 μm	AC % ≤1 μm
0	24	22	23	26
20	32	26	40	42
60	59	58	70	79
100	94	74	93	95

Each result is for the combination of low and high fiber density slides; all laboratories included. Key as Table 1.

is also consistent with workplace air samples of amphibole asbestos (again see review in Harper *et al.*, 2008 and, particularly, Gibbs and Hwang, 1980; Virta *et al.*, 1983). Because of these overlaps, no parameter based on length can be used to effectively differentiate these particles. On the other hand, the simple parameter of width does a remarkably effective job of differentiating the different slides in the correct order of presumed asbestos content, for all the laboratories that had no 'bias' in making this measurement. In fact, with the notable exception of laboratory #2, when 1 μm width is used as the criterion for asbestos, a slide that nominally is expected to contain <50% asbestos would likely be declared to contain <50% asbestos, while a slide that nominally is expected to contain >50% asbestos would likely be declared to contain at least that much. (It should be further noted that the use of the RIB graticule brought the results for laboratory #9 for the amosite/grunerite slides into concordance with those of the other laboratories.) There exists an overlap in the size range of cleavage fragments that would cause ∼20% of cleavage fragments in this study ≤1 μm to be thought of as asbestos. This drops to almost zero if a width criterion of ≤0.5 μm is used. The percentage of actinolite asbestos and tremolite asbestos fibers >0.5 μm width for all fibers in the materials used for this study measured at RTI International by phase-contrast microscopy with the Walton–Beckett graticule were 7.3 and 8.5%, respectively. Therefore, the likelihood of reporting 20% of cleavage fragments as asbestos could be replaced by a likelihood of reporting a significant fraction of asbestos as cleavage fragments by using 0.5 μm as the cut-off in place of 1 μm. Thus, it seems likely that a width cut-off in the range 0.5–1 μm would be a rational means of separating likely asbestos fibers from likely cleavage fragments in a screening method. When the distribution of widths of the particles selected for this study in the slides containing only 100% asbestos fibers or 100% cleavage fragments are graphed, the valley between the distributions occurs at ∼0.84 μm, which is close enough to 1.0 μm to make little difference. The percentage of fibers classified as asbestos or non-asbestos for each nominal asbestos proportion, expressed as an average of the low and high loading slides, is shown in Table 4 for 1 μm width (the nearest whole number).

DISCUSSION

In the ASTM D7200 Standard, an asbestos fraction >50% at an airborne concentration of half the applicable limit value would result in a requirement for further analysis by alternative techniques, such as electron microscopy. From this study, considering populations whose asbestos fiber content is greater than ∼25%, the magnitude of the bias in discrimination is minimized, and the accuracy (including variability as well as bias) is consistent with the ability to make a research decision regarding concentration of fibers or fragments with width ∼1 μm (Appendix 1) as per the procedure in ASTM D7200.

A question remains as to whether discrimination by any specified width can be used for actual airborne samples or whether it is an artifact of the laboratory sample preparation process. Schneider *et al.* (1998) suggested aspect ratio was important but found that an aspect ratio of 8:1 excludes most cleavage fragments without excluding ≥10% of the asbestos fibers, but this is no better than the results for '100% asbestos' provided by the width-only criteria in Table 4. Van Orden *et al.* (2009) carried out a laboratory study of asbestos and non-asbestos amphibole particle sizes. They reported a three-step

sample preparation procedure, beginning with the removal of a suspension from shaking samples in water (but it is assumed that there must have been a sample reduction step prior to this to render at least non-asbestos materials in a state where material would come loose on shaking with water). They then added more water to the remaining material and sonicated it and again removed the suspension. Finally, they crushed the remainder and sieved it and then suspended and sonicated again. It appears from the text of their procedure that each of the three resulting materials was examined separately under the microscope, but the results were combined for statistical analyses. With this preparation, the four minerals assumed to be non-asbestiform amphiboles (Gouverneur tremolite, West Greenland anthophyllite, Homestake cummingtonite-grunerite, and Shinness tremolite) gave fibers as defined above where typically more than half were <1 μm wide (49–69%). In that study, a width parameter of 0.5 μm would certainly have been a better discriminator than 1 μm since 10–38% of fibers from these minerals were also <0.5 μm wide. This is rather thinner than the cleavage fragments produced in our study. The authors justify their size distribution by reference to airborne samples analyzed by Virta *et al.* (1983), but the data in that reference for mine samples are for particles of any length visible under scanning electron microscope with an aspect ratio $\geq$2:1, which is probably not the same as if they had only counted fibers >5 μm long with an aspect ratio $\geq$3:1.

Data on transmission electron microscopy measurements of supposed tremolite cleavage fragments meeting NIOSH 'A' rules criteria for counting in three air samples from different locations within the RT Vanderbilt talc processing plant in Gouverneur, NY, were provided for comparison (J. Kelse, personal communication). For particles >10 μm, very few were also <1 μm wide, but for particles in the range 5–10 μm length, which were the majority, a relatively large proportion (30–36%) were <1 μm wide. Therefore, the overall proportion <1 μm wide was 22–27%, which is more in line with the results from this ILS. It was also clear that even fewer of the shorter cleavage fragments were <0.5 μm wide, which does lend support to the use of this value to fully exclude cleavage fragments, although it likely also will exclude some asbestos fibers. Kenny *et al.* (1987) had examined amosite fibers under both electron microscopy and phase-contrast microscopy. All fibers examined were <1.0 μm wide, even with lengths up to 20 μm. Interestingly, almost all fibers >5 μm long were visible under phase-contrast microscopy, even for width down to 0.0625 μm, which is consistent with the 0.15 μm width limit for visibility of chrysotile fibers found by Rooker *et al.* (1982). A personal air sample filter, which had been collected during excavation of the tremolite asbestos used in this study was received by our laboratory and evaluated according to particle width. Of 127 fibers examined under phase-contrast microscopy, 85% were thinner than 1 μm. A number of personal air sampling filters were also obtained from work on the demolition of the Powhatan asbestos mill in Maryland, USA. The fibers (previously identified as anthophyllite asbestos) on three filters that had $\geq$25 fibers per 100 fields were found to be 72, 92, and 99% <1 μm wide. Finally, we can also compare our data to that from air samples of fibrous amphibole generally considered to be asbestiform in the air of the vermiculite processing plant in Libby Montana. Amandus *et al.* (1987) found only 7% of particles under phase-contrast microscopy to be >0.88 μm width.

Van Orden *et al.* (2009) combined their laboratory-generated width data with aspect ratio according to a procedure (the 'Chatfield procedure') that has been presented at a conference (Chatfield, 2008) but not yet published in the peer-reviewed literature. This procedure combines aspect ratio with width to determine asbestiform from non-asbestiform particles. If this procedure is applied to the fibers in our study, a $\geq$10:1 aspect ratio (but not 20:1 as Chatfield suggested as this would miss many asbestos fibers) coupled with a width criterion between 0.5 and 1 μm would also provide an appropriate discrimination. However, the percentages of fibers on each slide determined to be asbestos by this method were found to be almost identical to those determined using a simpler width-only criterion.

The possibility exists that any value for width selected for the purpose of discrimination may be an artifact of the sample preparation procedure. It must further be kept in mind that there are situations where the determination of asbestos versus non-asbestos for a single particle cannot be made with confidence whatever the width since wide asbestos bundles do occur, as do thin cleavage fragments. Hence, discrimination should only be based on a reasonably large population of particles.

CONCLUSIONS

It has been clearly shown that the procedure for discriminating asbestos from cleavage fragments and prismatic crystals as currently included in ASTM Standard D7200 was not effective across all participating laboratories when applied to the

amphibole asbestos and cleavage fragments prepared for this ILS. The recognition of Class 1 characteristics of asbestos (fibrillar bundling, split ends, and curvature) was highly variable among laboratories, and the existence of these characteristics appears to be anyway dependent on particle length and type of asbestos. While features specific to asbestos may be an important guide to the presence of asbestos when properly recognized, it does not appear that such a classification can be applied quantitatively across all laboratories, at least without additional training. Class 1 characteristics could still be included in D7200, however, because the excessive recognition of cleavage fragments by some laboratories leads to a conservative decision to require additional investigation. The procedure in ASTM D7200 is for further analysis when the concentration of airborne fibers is greater than an applicable action level and when $\geq$50% of these fibers appear to be asbestos by discrimination under the phase-contrast microscope, and thus, any criteria adopted for discrimination under optical microscopy will be confirmed through additional techniques. Class 2 parameters were ineffective in discrimination because of the excessive overlap in length between asbestos fibers and cleavage fragments in our study in the 5–15 μm length range. Published and unpublished data suggest that this overlap also occurs with airborne fibers found in occupational environments. Finally, it has been demonstrated with these laboratory samples that a remarkably effective discrimination is possible using only a single measurement of width, somewhere between 0.5 and 1.0 μm. A criterion of $\leq$0.84 μm gives the best overall discrimination, although $\leq$1.0 μm gives the fewest false negatives for asbestos fibers (Table 4). It has been further demonstrated that where some laboratories differ from others in their ability to measure around this dimension with the Walton–Beckett graticule, they may improve their ability to do so when using the RIB graticule, although this may not be sustainable if it is only a psychological effect of the novelty of the new graticule. (Note that the equivalency of fiber 'counts' has not been established between the Walton–Beckett and RIB graticule, but it is unlikely that they will be radically different). The authors are simply reporting a finding from the ILS that width could be used to discriminate amphibole asbestos fibers from non-asbestos cleavage fragments under phase-contrast microscopy to support a decision as to whether further analysis is required. The authors do not suggest that any width parameter be used as an indication of toxicity without consensus agreement based on compelling evidence. It is likely that this same finding would apply also to chrysotile asbestos and serpentine mineral cleavage fragments, but this has not been tested.

FUNDING

The inter-laboratory study was funded internally by the National Institute for Occupational Safety and Health through a Public Health Practice Project grant (Project 927Z8UQ Improvements in Assessing Exposures to Fibers in Mining). Dr David Bartley received compensation for consultation from this project and from the American Society for Testing and Materials fund for Inter-Laboratory Studies. RTI International was contracted to provide the materials for the study from the NIOSH PHP project and from a prior NIOSH National Occupational Research Agenda (NORA) Pilot Project.

Acknowledgements—The authors are sincerely thankful for all the participating laboratories that contributed their time and efforts without recompense. The authors are grateful to Paul Middendorf and Joseph Fernback (NIOSH) and Dan Crane (OSHA) for reviewing this manuscript prior to journal submission.

Disclaimer—The findings and conclusions in this report are those of the authors and do not necessarily represent the official position of the Centers for Disease Control and Prevention.

APPENDIX 1: Uncertainty issues

Plan

Calculated here is the uncertainty in estimated fiber or cleavage fragment concentrations, distinguishing fiber versus fragment simply by a value for discrimination by width. The approach taken is to compute the within-laboratory 'symmetric accuracy range' *A*, defined as the percent range about accepted values containing 95% of estimates. Defined as such, *A* is a measure of the measurement error, accounting for both imprecision and systematic error. The accuracy range *A* has been exploited for several decades in the evaluation of sampling and analytical methods applied in industrial hygiene (Busch, 1977; NIOSH, 2003). The accuracy range *A* also has been found to be a useful auxiliary function in approximating prediction intervals for justifying current worldwide policy in characterizing uncertainty in measurement (ISO GUM, 1995; Bartley, 2001, 2008).

The plan for the following sections is to first compute the imprecision in width estimates on the basis of the round robin described in the text. Second, the disparate width distributions of fibers and fragments are estimated. The dependence of fiber and

fragment concentration estimate accuracy range on the distributions and on the width measurement imprecision is determined formally. This dependence leads to an optimal width discrimination value. Finally, an explicit map of accuracy range A is given in terms of the (fiber or fragment) object fraction and mean number. Additionally, the inter-laboratory imprecision in fiber or fragment width measurement is estimated by simulation.

Within- and between-laboratory width measurement imprecision

With width proposed for distinguishing cleavage fragments from fibers, the accuracy of measurement by visual comparison to the separation of lines etched on a graticule is an important characteristic of the method. The measurement of width smaller than a few micrometers is below the 'limit of quantification', where the (relative) imprecision is not a constant and indeed may become large with decreasing true width. Nevertheless, the imprecision can be specified for widths near the proposed decision point, for example, near 1 μm. Naturally, if the fiber and fragment distributions are widely separated, then high width accuracy is not needed for estimating object concentration.

A large number N (several thousand) of width measurements relative to laboratory averages (as the consensus widths) of several hundred fibers or fragments within $\bar{w} \pm 0.1\,\mu\text{m}$, where $\bar{w}$ is fixed at 0.5 and 1.0 μm, were analyzed [discarding at the 3σ level a small number (<0.5%) of measurements as outliers]. The ratio r_{lf} of any width measurement relative to consensus was modeled as:

$$r_{lf} = 1.00 + \left(\sigma_b \varepsilon_l + \sigma_w \varepsilon_{lf}\right)/\bar{w}, \tag{A.1}$$

where $l = 1, \ldots, L\ (= 11)$ designates a laboratory, and $f = 1, \ldots, F[11]$ denotes a fiber or fragment, with $F[l]$ the number analyzed by the lth laboratory. The quantities ε_l and ε_{lf} are independent standard normal random variables, and therefore, σ_b and σ_w are the between-laboratory and within-laboratory standard deviations dependent on mean width $\bar{w}$. See Fig. A1 for a graphical depiction of the data.

The quantities σ_b and σ_w may be estimated through a 'one-way' ANOVA with unbalanced data. For details, see Sahai and Ojeda (2005). "'Unbalanced' means that the number $F[l]$ of widths measured depends on l, varying greatly from laboratory to laboratory, from ~1 to 300. It was necessary to account for imbalance as 10 of 11 laboratories analyzed actinolite and tremolite objects, whereas only 9 (and not all overlapping) analyzed amosite/grunerite (AG) and crocidolite/riebeckite (CR).

The ANOVA is carried out in terms of the following sums of squares:

$$\begin{aligned} \mathrm{SS}_{\text{total}} &\equiv \sum_{l=1}^{L} \sum_{f=1}^{F[l]} \left(r_{fl} - \bar{r}\right)^2 \quad (d.f. = N - 1) \\ &= \mathrm{SS}_b + \mathrm{SS}_w, \end{aligned} \tag{A.2}$$

where SS_b and SS_w are given by

$$\begin{aligned} \mathrm{SS}_w &\equiv \sum_{l=1}^{L} \sum_{f=1}^{F[l]} \left(r_{fl} - r_{\cdot l}\right)^2 \quad (d.f. = N - L), \\ \mathrm{SS}_b &\equiv \sum_{l=1}^{L} F\left[l\right] \left(r_{\cdot l} - \bar{r}\right)^2 \quad (d.f. = L - 1). \end{aligned} \tag{A.3}$$

The quantities $r_{\cdot l}$ are the laboratory means, and $\bar{r}$ is the mean over all N measurements (which does not equal the mean of the laboratory means in the case of unbalanced data).

The variance estimates s_w^2 and s_b^2 are obtained by solving:

$$\begin{aligned} s_w^2 \Big/ \bar{w}^2 &\equiv \mathrm{SS}_w \Big/ \left(N - L\right), \\ \left(s_w^2 + n_0 s_b^2\right) \Big/ \bar{w}^2 &\equiv \mathrm{SS}_b \Big/ \left(L - 1\right), \end{aligned} \tag{A.4}$$

defined so that expected values are correct. The number n_0 is peculiar to unbalanced data and is calculated as:

$$n_0 \equiv \frac{N^2 - \sum_{l=1}^{L} F[l]^2}{N(L-1)}. \tag{A.5}$$

Result. The standard deviations were estimated via equation (A.4) for width measurements near 0.5 μm and also near 1.0 μm. The results are as follows:

From 3220 width measurements near 0.5 μm of 342 fibers or fragments by 11 laboratories,

$$\begin{aligned} s_w &= 0.18\,\mu\text{m}, \\ s_b &= 0.17\,\mu\text{m}. \end{aligned} \tag{A.6}$$

From 2546 width measurements near 1.0 μm of 274 fibers or fragments by 11 laboratories,

$$\begin{aligned} s_w &= 0.26\,\mu\text{m}, \\ s_b &= 0.20\,\mu\text{m}. \end{aligned} \tag{A.7}$$

Note that the standard deviation depends only weakly on width, consistent with the width measurements taken here well below the limit of quantification.

Fiber and fragment width distributions

Besides width measurement uncertainty, the width distributions of both fibers and fragments are needed

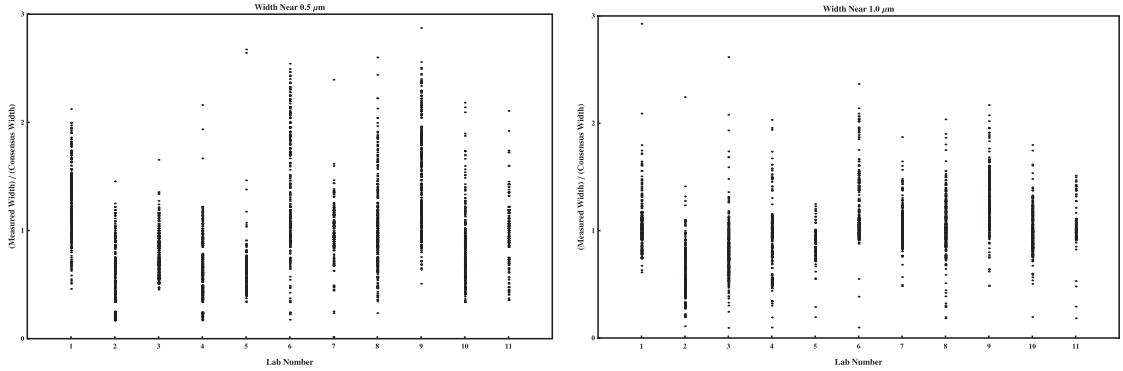

Figure A1. Measured widths of fibers or fragments in (0.4 and 0.6 mm) and in (0.9 and 1.1 mm). Each point represents the ratio of an individual measurement of a particle to the inter-laboratory mean value for that particle.

in order to make rough estimates of the accuracy range for fiber concentration estimates. The width distributions of fibers and fragments are taken from the AG and CR laboratory consensus data from 100% asbestos fibers or 100% cleavage fragments. Figure A2 shows log-normal fits to the two distributions. The fitted median widths, mw, and geometric standard deviations, gsd, are found to be:

$$(\text{mw, gsd}) = \left\{ \begin{array}{l} (1.49\ \ \mu\text{m, } 1.7), \text{ fragments} \\ (0.42\ \ \mu\text{m, } 1.8), \text{ fibers} \end{array} \right\}. \tag{A.8}$$

Bias and imprecision of concentration estimates in terms of distribution overlap and width measurement uncertainty

Suppose an air sample of volume V is taken and is found to contain $\hat{N}$ fibers or fragments, where the (Poisson) sampling error is characterized by $\text{Var}[\hat{N}]=N$, the mean number to be found in V. Let $\alpha_\pm$ represents the unknown true (population mean) fractions and $\text{LN}_\pm$ the (log-normal) width distributions of $\left\{ \begin{array}{l} \text{fragments} \\ \text{fibers} \end{array} \right\}$ specified in equation (A.8). Fibers are denoted by $-$ and fragments by $+$. Let $N[w - w', \sigma_\text{w}]$ represents the normal distribution of measurements w about consensus value w' with standard deviation σ_w [evaluated at w' using equations (A.6 and A.7)]. Let w_c represents the width measurement discrimination value below which a fiber or a fragment is counted as a fiber.

Then, the probability $d\pi_\pm$ that the object is a fragment or a fiber arising from within dw' of w' is

$$d\pi_\pm = \alpha_\pm \text{LN}_\pm[w']dw'. \tag{A.9}$$

The probability dP_- that this particle will be counted as a fiber is then

$$\begin{aligned} dP_- &= \int_{-\infty}^{w_\text{c}} dw\ N[w - w', \sigma_w]d\pi_- \\ &\quad + \int_{-\infty}^{w_\text{c}} N[w - w', \sigma_w]d\pi_+. \end{aligned} \tag{A.10}$$

Summing probabilities corresponding to alternative width sources w', then gives the probability P_- for counting a single object (correctly or not) as a fiber:

$$\begin{aligned} P_- &= \alpha_- \textstyle\int_{-\infty}^{w_c} dw \int_0^\infty dw' N[w - w', \sigma_\text{w}]\text{LN}_-\left[w'\right] \\ &\quad + \alpha_+ \textstyle\int_{-\infty}^{w_c} dw \int_0^\infty dw' N[w - w', \sigma_w]\text{LN}_+\left[w'\right] \\ &= \textstyle\int_{-\infty}^{w_c} dw \int_0^\infty dw' N[w - w', \sigma_\text{w}]\left(\alpha_-\text{LN}_-\left[w'\right]\right. \\ &\quad \left. + \alpha_+\text{LN}_+\left[w'\right]\right). \end{aligned} \tag{A.11a}$$

The probability P_+ for counting a single object as a fragment is then also determined as:

$$P_+ = 1 - P_-. \tag{A.11b}$$

The binomial distribution then gives the number $\hat{n}_\pm$ of the N objects counted (correctly or not) as fragments or fibers with:

$$\begin{aligned} E[\hat{n}_\pm] &= P_\pm \hat{N}, \\ \text{Var}[\hat{n}_\pm] &= P_\pm(1 - P_\pm)\hat{N}. \end{aligned} \tag{A.12}$$

Therefore,

$$\hat{n}_\pm = P_\pm \hat{N} + \hat{\varepsilon}\sqrt{P_\pm(1 - P_\pm)\hat{N}}, \tag{A.13}$$

where $E[\hat{\varepsilon}]=0$, $\text{Var}[\hat{\varepsilon}]=1$, and $\hat{\varepsilon}$ and $\hat{N}$ are uncorrelated. Approximating $\hat{N}$ by the mean $\hat{N}$ in the second term gives

$$\hat{n}_\pm \approx P_\pm \hat{N} + \hat{\varepsilon}\sqrt{P_\pm(1 - P_\pm)N}, \tag{A.14}$$

and thus, $\text{Var}[\hat{n}_\pm]$ simplifies to a Poisson distribution dependence on N as

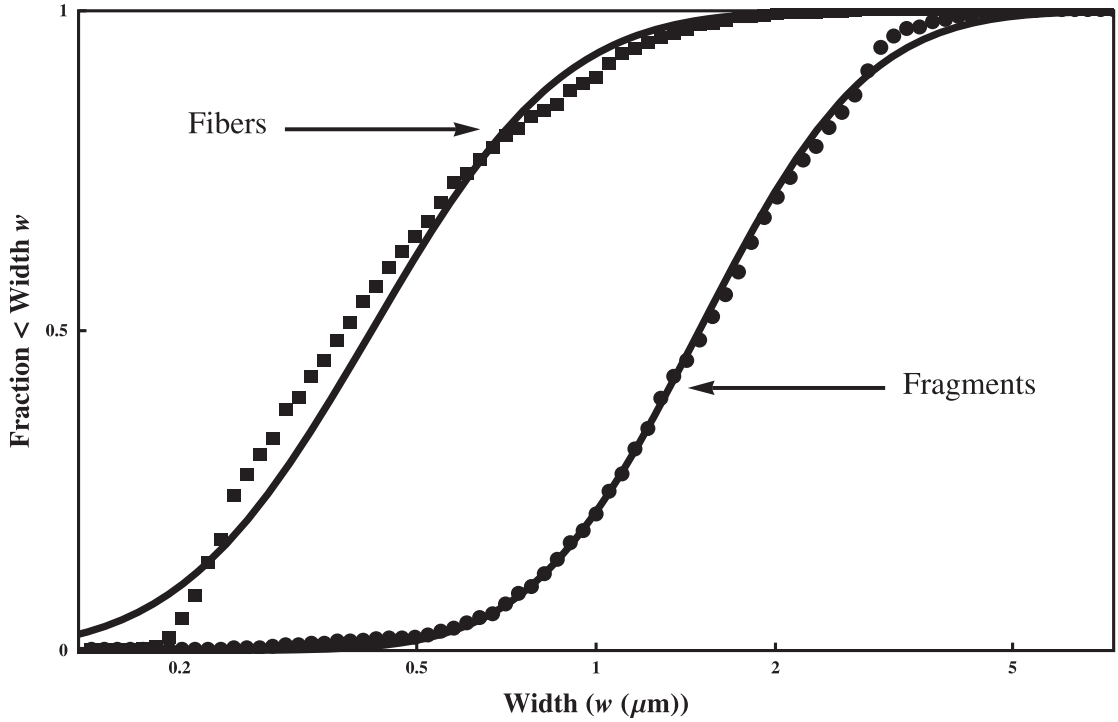

Figure A2. Cumulative width distributions for AG and CR fibers (squares) and fragments (circles). Each point represents a bin of laboratory consensus width measurements within 0.05-μm intervals. Also, shown are log-normal fits (solid curves) to the data.

$$\begin{aligned}\mathrm{Var}[\hat{n}_\pm] &\approx P_\pm^2 N + P_\pm(1 - P_\pm)N \\ &= P_\pm N.\end{aligned} \tag{A.15}$$

The true relative standard deviation $\mathrm{TRSD}_\pm$ is then given by:

$$\begin{aligned}\mathrm{TRSD}_\pm^2 &\equiv \mathrm{Var}[\hat{n}_\pm]/n_\pm^2 \\ &= (1 + \Delta_\pm)/n_\pm,\end{aligned} \tag{A.16}$$

with the mean bias $\Delta_\pm$ defined as:

$$\begin{aligned}\Delta_\pm &\equiv (E[\hat{n}_\pm] - n_\pm)/n_\pm \\ &= P_\pm/\alpha_\pm - 1.\end{aligned} \tag{A.17a}$$

Now $\Delta_\pm$ can be expressed as

$$\begin{aligned}\Delta_- &= +I_- + (\alpha_-^{-1} - 1)I_+ - 1, \\ \Delta_+ &= -I_+ - (\alpha_+^{-1} - 1)I_- - 1 + \alpha_+^{-1},\end{aligned} \tag{A.17b}$$

where I_+, the fiber false positive rate, and I_-, complement of the fragment false positive rate, are the two dimensionless integrals in equation (A.11), evaluated numerically:

$$I_\pm \equiv \int_0^{w_c} dw \int_0^\infty dw' N[w - w', \alpha_w]\mathrm{LN}_\pm[w']. \tag{A.18}$$

Note that if a laboratory employs multiple counters whose measurements are significantly biased relative to each other or if inter-laboratory bias is to be considered, then an additional contribution of the form $\sigma_0^2/n_\pm^2 + S_r^2$ would be added to the expression of equation (A.16). In addition to a Poisson contribution as in equation (A.16), Ogden (1982) used a single extra constant S_r^2, a true relative standard deviation component squared, to characterize inter-counter bias on implementing a specific set of asbestos counting rules. Such bias would depend on practices in place at a given laboratory.

Optimal width discrimination value

An optimal width discrimination value, w_c, may be selected by the following argument. The bias in both fiber and fragment concentrations decreases with the fiber or fragment fraction. For example, when a fraction is zero, there exists positive bias if the complementary width distribution is positive on both sides of w_c. If a fraction is 100%, then similarly the bias is 'negative'. Furthermore, at any particular value for either fraction, the bias in fiber (or fragment) concentration estimates increases (or decreases) with w_c. Therefore, a balanced and minimum bias is obtained by choosing w_c so that the two biases are equal. Remarkably, the cut-off w_c can be chosen so that the two biases can be made equal over the entire range of their object fractions

(from 0 to 100%). Equation (A.17b) directly implies that the biases are equal if w_c is selected so that

$$I_- + I_+ = 1 (\Leftarrow \Delta_+ = \Delta_-). \quad \text{(A.19)}$$

In other words, w_c is set so that the false-negative and positive rates are both equal to I_+.

In this case, the (equal) biases Δ can be represented (equation A.17b) in terms of object fraction α simply as

$$\Delta = (\alpha^{-1} - 2) I_+ . \quad \text{(A.20)}$$

Note that Δ is zero when a fraction is 50% and would vanish for all object fractions from 0 to 100% if I_+ is zero, meaning no overlap in the width distributions. Analogous to equation (A.20), TRSD (equation A.16) may be written in terms of the object number n as

$$\text{TRSD} = \sqrt{(1 + \Delta)/n}, \quad \text{(A.21)}$$

dependent on the sample size or sampled volume V, unlike the bias Δ.

Result. Using the size distributions specified in equation (A.8), numerical solution of $\Delta_+ = \Delta$, taking σ_w as the value at w_c by interpolating between equations (A.6 and A.7), results in optimal width discrimination value and error rate I_+:

$$\begin{aligned} w_c &= 0.84\ \mu\text{m}, \\ I_+ &= 16\%. \end{aligned} \quad \text{(A.22)}$$

Accuracy range

Finally, the combined effect of bias Δ and imprecision TRSD may be expressed as the symmetric accuracy range A defined as the percent range containing 95% of the width measurements about true values. In normal approximation, A in terms of Δ and TRSD may be determined from the cumulative normal function Φ by numerical solution of

$$\Phi[(A + \Delta)/\text{TRSD}] - \Phi[(A - \Delta)/\text{TRSD}] = 95\%. \quad \text{(A.23)}$$

The function $A[\Delta, \text{TRSD}]$ may also be determined in terms of other statistical functions (Krishnamoorthy and Mathew, 2009) or by approximation (Bartley, 2001) accurate not only in the limits $\Delta \to 0$ or $|\Delta| \gg \text{TRSD}$ as

$$A = \begin{cases} 1.960 \times \sqrt{\Delta^2 + \text{TRSD}^2}, & \text{if } |\Delta| < \text{TRSD}/1.645, \\ |\Delta| + 1.645 \times \text{TRSD}, & \text{otherwise.} \end{cases} \quad \text{(A.24)}$$

With the above expressions (equations A.20 and A.21) for bias and imprecision, the accuracy range A is a function of the object fraction α and the sampled object number n. This function is plotted in Fig. A3 as a contour diagram for width cut-size, $w_c = 0.84$ (equation A.22).

Note that the accuracy ranges depicted in Fig. A3 are expressed relative to accepted object (fiber or fragment) fraction. The aim is for interpreting research results, and as such, this definition differs

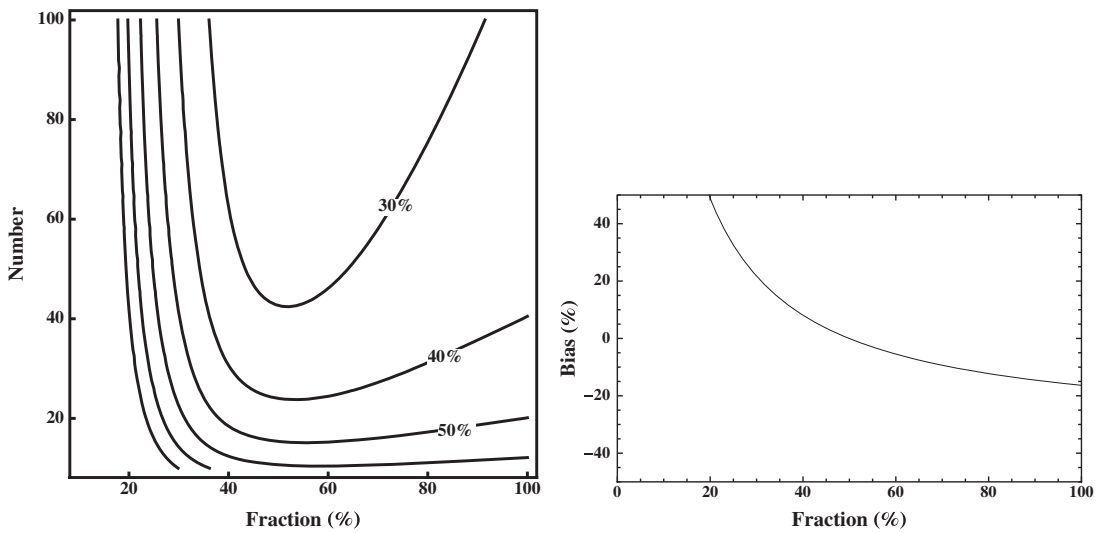

Figure A3. Accuracy range and bias of concentration estimates in terms of object number and fraction for optimal width discrimination value of 0.84 μm. Note that the same graph applies to the fraction and number of asbestos fibers and fraction and number of cleavage fragments at the optimal width discrimination value.

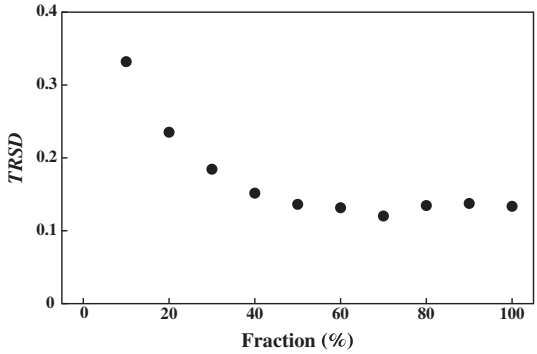

Figure A4. Between-laboratory TRSD in the fiber (or fragment) concentration estimate versus the unknown fraction of fiber (or fragment) for optimal width discrimination value of 0.84 μm.

from that used in the established (NIOSH, 2003b) target criterion of 25% for within-laboratory uncertainty, generally referring to sampling and analytical variations relative to a 'standard'. The purpose in this case is to ensure fairness in decisions. In the case of asbestos, the standard could refer to the consensus number concentration of fibers or fragments <0.84 μm (for example). The (within-laboratory) accuracy range would be expressed relative to this quantity rather than the accepted object fraction and, in behaving as $1.960/\sqrt{n}$ without bias, would not exhibit the extreme values at low asbestos concentration as seen in Fig. A3.

Aside from the within-laboratory accuracy range, the between-laboratory imprecision is also a significant characteristic of the method. This imprecision cannot be decreased by increasing the sampling volume. See also the discussion following equation (A.18). Following equation (A.7), the between-laboratory total relative standard deviation TRSD can be estimated. Results obtained by simulation are shown in Fig. A.4.

REFERENCES

Amandus HE, Wheeler R, Jankovic J *et al*. (1987) The morbidity and mortality of vermiculite miners and millers exposed to tremolite-actinolite: part I. Exposure estimates. Am J Ind Med; 11: 1–14.

ASTM International. (2006) Standard practice for sampling and counting airborne fibers, including asbestos fibers, in mines and quarries, by phase contrast microscopy and transmission electron microscopy. D7200-06. West Conshohocken, PA: American Society for Testing and Materials.

Bartley DL. (2001) Definition and assessment of sampling and analytical accuracy. Ann Occup Hyg; 45: 357–64.

Bartley DL. (2008) The meaning of the bias uncertainty measure. Ann Occup Hyg; 52: 519–25.

Brattin W, Orr J. (2004) Analysis of asbestos in soil by transmission electron microscopy following water sedimentation fractionation, Libby Superfund Site standard operating procedure (SOP) EPA-Libby-07, rev. 3. Denver, CO: US environmental Protection Agency, Region 8.

Busch KA. (1977) Standards completion program statistical protocol. In Taylor DG, Kupel RE and Bryant JM, editors. Documentation of the NIOSH validation tests. Cincinnati, OH: U.S. Department of Health, Education, and Welfare (DHEW), Centers for Disease Control (CDC), National Institute for occupational Safety and Health (NIOSH), [DHEW (NIOSH) Publ. No. 77–185]. pp. 7–12.

Chatfield EJ. (2008) A procedure for quantitative description of fibrosity in amphibole minerals. Paper presented at the ASTM International 2008 Johnson conference: Critical issues in monitoring asbestos, Burlington, VT, July 14–18, 2008.

EPA. (2003) Report on the peer consultation workshop to discuss a proposed protocol to assess asbestos-related risk, final report. Washington, DC: US United states environmental Protection Agency, Office of solid Waste and Emergency Response. pp. viii.

Gibbs GW, Hwang CY. (1980) Dimensions of airborne asbestos fibers. Biological effects of mineral fibers. Lyon, France: IARC Science Publications 30; pp. 69–78.

Harper M, Lee EG, Doorn SS *et al*. (2008) Differentiating nonasbestiform amphibole and amphibole asbestos by size characteristics. J Occup Environ Hyg; 5: 761–70.

Harper M, Lee EG, Harvey B *et al*. (2007) The effect of a proposed change to fiber-counting rules in ASTM International Standard D7200-06. J Occup Environ Hyg; 4: D42–5.

ISO GUM. (1995) Guide to the expression of uncertainty in measurement, ISO Guide 98. Geneva, Switzerland: International Organization for Standardization.

Kenney LC, Rood AP, Blight BJN. (1987) A direct measurement of the visibility of amosite asbestos fibres by phase contrast optical microscope. Ann Occup Hyg; 33: 261–64.

Krishnamoorthy K, Mathew T. (2009) Inference on the symmetric-range accuracy. Ann Occup Hyg; 53: 167–71.

MSHA. (2005) Mine Safety and Health Administration: asbestos exposure limit; proposed rule. U.S. Federal Registry, FR July 29, 2005, pp. 43950–89.

NIOSH (2003a) Method 7400, asbestos and other fibers by PCM. Issue 2 (8/15/94). In Schlecht PC and O'Connor PF, editors. NIOSH manual of analytical methods. 4th edn DHSS (NIOSH) Pub. No. 2003-154. Cincinnati, OH: National Institute for Occupational Safety and Health.

NIOSH. (2003b) Measurement uncertainty and NIOSH method accuracy range, Chapter P. In Schlecht PC and O'Connor PF, editors. NIOSH manual of analytical methods. 4th edn. (Suppl 3), DHHS (NIOSH) publication No. 2003-Cincinnati, OH: National Institute for Occupational Safety and Health.

NIST. (1991) Certificate. Standard reference material 1866A: common commercial asbestos. Gaithersburg, MD: US Department of Commerce: National Institute of Standards and Technology.

Ogden TL. (1982) The reproducibility of asbestos counts. HSE research paper 18. Cricklewood, UK: Health and Safety Executive.

OSHA. (1988, revised 1997) Method ID-160, asbestos in air. In Dane Crane, editor. OSHA manual of sampling and analytical methods. Sandy, UT: US Department of Labor: Occupational Safety and Health Administration Salt Lake Technical Center. Available at http://www.osha.gov/dts/sltc/methods/inorganic/id160/id160.html.

OSHA. (1992) Occupational Safety and Health Administration: occupational exposure to asbestos, tremolite, anthophyllite and actinolite, preamble to final rule, section 5-V. Health Effects. US Federal Registry, 57 FR 24310, June 8, 1992.

Rooker SJ, Vaughan NP, Le Guen JM. (1982) On the visibility of fibers by phase contrast microscopy. Am Ind Hyg Assoc J; 43: 505–15.

Sahai H, Ojeda MM. (2005) Analysis of variance for random models: unbalanced data. Boston, MA: Birkhäuser.

Schneider T, Davies LST, Burdett G *et al*. (1998) Development of a method for the determination of low contents of asbestos fibres in bulk material. Analyst; 123: 1393–400.

Van Orden DR, Lee RJ, Allison KA *et al*. (2009) Width distributions of asbestos and non-asbestos amphibole minerals. Indoor Built Environ; 18: 531–40.

Virta RL, Shedd KB, Wylie AG *et al*. (1983) Size and shape characteristics of amphibole asbestos (amosite) and amphibole cleavage fragments (actinolite, cummingtonite) collected on occupational air monitoring filters. Chapter 47. In Marple VA and Liu BYH, editors. Aerosols in the mining and industrial work environments, vol 2: characterization. Ann Arbor, MI: Ann Arbor Science; pp. 633–43.

WHO. (1997) Determination of airborne fibre number concentrations; a recommended method, by phase contrast optical microscopy (membrane filter method). Geneva, Switzerland: World Health Organisation.